Chair of Structural Analysis
Technical University of Munich

A Nitsche-type method for the multipatch coupling and the application of weak Dirichlet boundary conditions in transient nonlinear isogeometric membrane analysis

Andreas Apostolatos*, Michael Breitenberger, Roland Wüchner and Kai-Uwe Bletzinger

Non-Uniform Rational B-Spline Basis Functions and Isogeometric Analysis

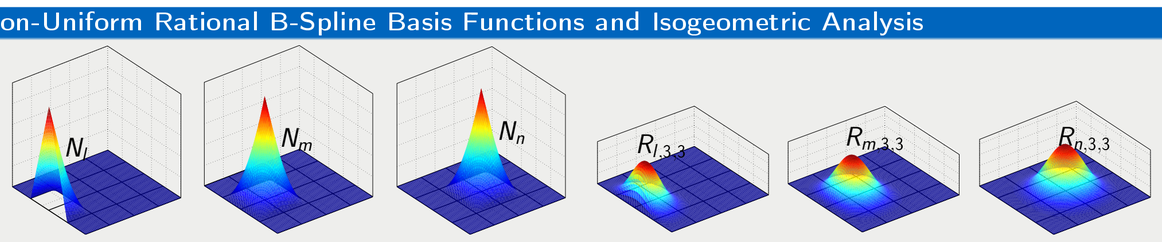

(a) Low order FEA basis functions (b) High order NURBS basis functions

Figure 1: Piece-wise polynomial basis functions

Classical Finite Element Analysis (FEA) uses typically C^0-continuous basis functions across the elements which also attain low polynomial order, see Figure 1(a), for numerically confronting Boundary Value Problems (BVPs).

On the other hand, Isogeometric Analysis (IGA), proposed first in [1], makes use of high order functions the so-called Non-Uniform Rational B-Spline (NURBS) basis functions which in addition may attain higher than C^0-continuity across the elements. Using the NURBS basis functions the low order basis functions can be also represented. The NURBS basis functions can be iteratively computed in 1D using the Cox-De-Boor formula:

$$N_{i,0}(\xi) = \begin{cases} 1 & \text{if } \xi \in [\xi_i, \xi_{i+1}[\\ 0 & \text{elsewhere} \end{cases}, \quad \text{and } N_{i,p}(\xi) = \frac{\xi - \xi_i}{\xi_{i+p} - \xi_i} N_{i,p-1}(\xi) + \frac{\xi_{i+p+1} - \xi}{\xi_{i+p+1} - \xi_{i+1}} N_{i+1,p-1}(\xi)$$

$$R_{i,p}(\xi) = \frac{N_{i,p}(\xi)}{\sum_{j=1}^{n} N_{j,p}(\xi)\, w_j}$$

where $\xi \in \Xi$, Ξ denotes the so-called knot vector of the NURBS patch, $N_{i,p}$, $R_{i,p}$ and w_i are the are the B-Spline basis functions, the corresponding NURBS basis functions and their weights, respectively. In more than one dimensions, the NURBS basis functions are constructed as a tensor product of the 1D basis functions.

Multipatch isogeometric membrane analysis

One of the main promises of IGA is the integration of design and analysis. Since the design models consist in principle of trimmed multipatches, methods have to be developed for imposing continuity constraints across the different patches. Those methods depend on the underlying BVP. In particular for the membrane problem [2] only continuity of the displacement field across the subdomains suffices in terms of the requirements of the corresponding variational form. Additionally, the membrane structures need to be subject into embedded cables at their free edges $\Gamma_c^{(i)}$ in order a unique static equilibrium state to be guaranteed. The variational form of the membrane problem without the continuity constraints writes; for each time instance $t \in \mathbb{T}$ find a $\mathbf{d} \in \boldsymbol{\mathcal{V}}_t$ such that,

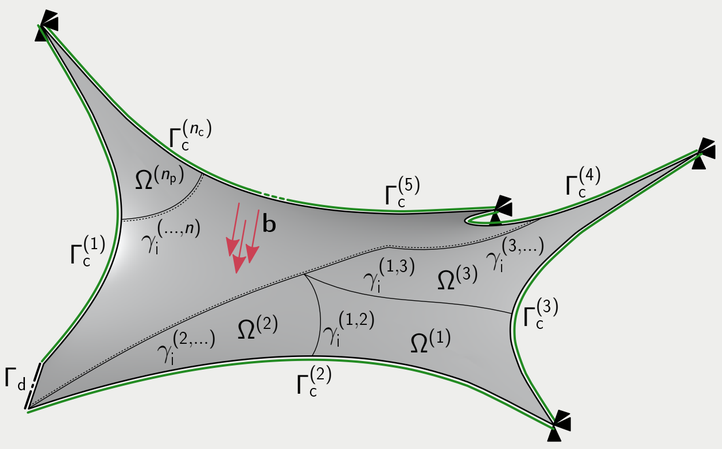

Figure 2: Multipatch membrane analysis

$$\left\langle \delta\mathbf{d}, \rho\ddot{\mathbf{d}} \right\rangle_{0,\Omega\setminus\gamma_i} + \left\langle \delta\mathbf{d}, c\dot{\mathbf{d}} \right\rangle_{0,\Omega\setminus\gamma_i} + a(\delta\mathbf{d}, \mathbf{d}) = l(\delta\mathbf{d}) \text{ for all } \delta\mathbf{d} \in \boldsymbol{\mathcal{V}}\,.$$

The inner products $\langle\cdot,\cdot\rangle_{0,\Omega\setminus\gamma_i} : \boldsymbol{\mathcal{V}} \times \boldsymbol{\mathcal{V}}$, the form $a : \boldsymbol{\mathcal{V}} \times \boldsymbol{\mathcal{V}} \to \mathbb{R}$ and the linear functional $l : \boldsymbol{\mathcal{V}} \to \mathbb{R}$ are defined as,

$$\left\langle \delta\mathbf{d}, \rho\ddot{\mathbf{d}} \right\rangle_{0,\Omega\setminus\gamma_i} := \int_{\Omega\setminus\gamma_i} \delta d_i^0\ \rho \ddot{d}_i^0\ \mathrm{d}\Omega\,,$$

$$a(\delta\mathbf{d}, \mathbf{d}) := \int_{\Omega\setminus\gamma_i} \delta d_i^0 \frac{\partial \varepsilon_{\alpha\beta}(\mathbf{d})}{\partial d_i^0} \left(n^{\alpha\beta}(\mathbf{d}) + n_0^{\alpha\beta} \right) \mathrm{d}\Omega + \int_{\Gamma_c} \delta d_i^0 \frac{\partial \widetilde{\varepsilon}(\mathbf{d})}{\partial d_i^0} \left(\widetilde{n}(\mathbf{d}) + \widetilde{n}_0 \right) \mathrm{d}\Gamma\,,$$

$$l(\delta\mathbf{d}) := \int_{\Omega\setminus\gamma_i} \delta d_i^0\ b_i^0\ \mathrm{d}\Omega\,,$$

Let $\mathsf{K}^{(i)}$ stand for the tangent stiffness matrix of patch $\Omega^{(i)}$. The coupled tangent stiffness matrix of the steady-state system at the $\hat{i}^{\text{th}}$ Newton-Rapshon iteration which also accounts for the weak enforcement of the Dirichlet boundary conditions can be formulated through various methods [3, 4] as shown below.

- Using the *Penalty* method:

$$\mathsf{K}\left(\hat{\mathbf{d}}\right) := \begin{bmatrix} \mathsf{K}^{(1)}\big|_{\hat{\mathbf{d}}^{(1)}} + \widetilde{\mathsf{K}}_{\widetilde{\beta}}^{(1)} + \overline{\mathsf{K}}_{\overline{\beta}}^{(1)} & \cdots & \overline{\mathsf{C}}^{(1,n)} \\ \vdots & \ddots & \vdots \\ \overline{\mathsf{C}}^{(n,1)} & \cdots & \mathsf{K}^{(n)}\big|_{\hat{\mathbf{d}}^{(n)}} + \widetilde{\mathsf{K}}_{\widetilde{\beta}}^{(n)} + \overline{\mathsf{K}}_{\overline{\beta}}^{(n)} \end{bmatrix}$$

- Using the *Lagrange Multipliers* method

$$\mathsf{K}\left(\hat{\mathbf{d}}\right) := \left[\begin{array}{cc|c|cc} \mathsf{K}^{(1)}\big|_{\hat{\mathbf{d}}^{(1)}} & \boldsymbol{\mathcal{M}}^{(1)} & \cdots & \mathbf{0} & \cdots\ \boldsymbol{\Lambda}^{(1,n)} \\ \left(\boldsymbol{\mathcal{M}}^{(1)}\right)^{\mathsf{T}} & \mathbf{0} & & & \\ \hline \vdots & & \ddots & \vdots & \ddots\ \vdots \\ \hline & & & \mathsf{K}^{(n)}\big|_{\hat{\mathbf{d}}^{(n)}} & \boldsymbol{\mathcal{M}}^{(n)} \\ \mathbf{0} & & \cdots & \left(\boldsymbol{\mathcal{M}}^{(n)}\right)^{\mathsf{T}} & \mathbf{0} \\ \hline \vdots & & \ddots & \vdots & \ddots\ \vdots \\ \left(\boldsymbol{\Lambda}^{(1,n)}\right)^{\mathsf{T}} & & \cdots & \left(\boldsymbol{\Lambda}^{(n,1)}\right)^{\mathsf{T}} & \cdots\ \mathbf{0} \end{array}\right].$$

- Using the *Nitsche* method:

$$\mathsf{K}\left(\hat{\mathbf{d}}\right) := \begin{bmatrix} \mathsf{K}^{(1)}\big|_{\hat{\mathbf{d}}^{(1)}} + \widetilde{\mathsf{K}}_{\mathsf{n}}^{(1)}\Big|_{\hat{\mathbf{d}}^{(1)}} + \overline{\mathsf{K}}_{\mathsf{n}}^{(1)}\Big|_{\hat{\mathbf{d}}^{(1)}} + \widetilde{\mathsf{K}}_{\widetilde{\beta}}^{(1)} + \overline{\mathsf{K}}_{\overline{\beta}}^{(1)} & \cdots & \overline{\mathsf{C}}^{(1,n)} \\ \vdots & \ddots & \vdots \\ \overline{\mathsf{C}}^{(n,1)} & \cdots & \mathsf{K}^{(n)}\big|_{\hat{\mathbf{d}}^{(n)}} + \widetilde{\mathsf{K}}_{\mathsf{n}}^{(n)}\Big|_{\hat{\mathbf{d}}^{(n)}} + \overline{\mathsf{K}}_{\mathsf{n}}^{(n)}\Big|_{\hat{\mathbf{d}}^{(n)}} + \widetilde{\mathsf{K}}_{\widetilde{\beta}}^{(n)} + \overline{\mathsf{K}}_{\overline{\beta}}^{(n)} \end{bmatrix}$$

The stabilization parameters $\widetilde{\beta}, \overline{\beta}$ in this case can be estimated piecewise for each Dirichlet and interface boundary as the maximum eigenvalues $\widetilde{\lambda}^{(i)}, \overline{\lambda}^{(i,j)}$ of the following eigenvalue problems such that a unique equilibrium state exists,

$$\det\left(\widetilde{\mathsf{Q}}_{\mathsf{n}}^{(i)}\left(\hat{\mathbf{d}}^{(i)}\right) - \widetilde{\lambda}^{(i)} \mathsf{K}^{(i)}\left(\hat{\mathbf{d}}^{(i)}\right) \right) = 0\,,$$

$$\det\left(\begin{bmatrix} \overline{\mathsf{Q}}_{\mathsf{n}}^{(i)}\left(\hat{\mathbf{d}}^{(i)}\right) & \overline{\mathsf{q}}_{\mathsf{n}}^{(i,j)}\left(\hat{\mathbf{d}}^{(i)}; \hat{\mathbf{d}}^{(j)}\right) \\ \overline{\mathsf{q}}_{\mathsf{n}}^{(j,i)}\left(\hat{\mathbf{d}}^{(i)}; \hat{\mathbf{d}}^{(j)}\right) & \overline{\mathsf{Q}}_{\mathsf{n}}^{(j)}\left(\hat{\mathbf{d}}^{(j)}\right) \end{bmatrix} + \overline{\lambda}^{(i,j)} \begin{bmatrix} \mathsf{K}^{(i)}\left(\hat{\mathbf{d}}^{(i)}\right) & \mathbf{0} \\ \mathbf{0} & \mathsf{K}^{(j)}\left(\hat{\mathbf{d}}^{(j)}\right) \end{bmatrix} \right) = 0\,.$$

The tangent stiffness matrix of the dynamic system can be then easily computed using the damping and the mass matrices in conjunction with the selected time integration method which within this study is the Bossak scheme.

Four-point sail

The benchmark problem of the form-finding analysis over a four-point sail of dimensions 10 m $\times$ 10 m is herein used for demonstrating the form-finding results using the Nitsche method for the multipatch coupling. Form-finding [5] is a method for finding the shape of static equilibrium with respect to the applied prestress. This shape ensures that the distribution of the stresses along the domain are such that a unique static equilibrium state exists. Additionally, cables are embedded into the sail at its four edges highlighted on Fig. 3 by green. The sail has Young's modulus $E = 210$ GPa and poisson ratio $\nu = 0.4$ whereas the applied prestress is assumed isotropic equal to $n_0 = 200$ KPa. Moreover, the Young's modulus and the prestress value for the cables is $\widetilde{E} = 210$GPa and $\widetilde{n}_0 = 2$ MN, respectively, for which the edges of the sail become arcs of a circle with given radius. In Fig. 3(b), 3(d) a comparison of the form-finding results when using a single and a 3-patch sail is given. Additionally, in Fig. 3(e) the evolution of the stabilization parameters for the multipatch coupling throughout the form-finding iterations is demonstrated. The stabilization parameters $\widetilde{\beta}$ and $\overline{\beta}$, for the application of weak Dirichlet boundary conditions and patch coupling, respectively, are estimated at each Dirichlet boundary and each interface by solving a set of eigenvalue problems. Those parameters converge asymptotically to a constant value as the form-found shape is obtained. A relatively high jump of the stabilization parameters is observed at the beginning of the form-finding iterations due to that large shape changes occur at the first form-finding iterations.

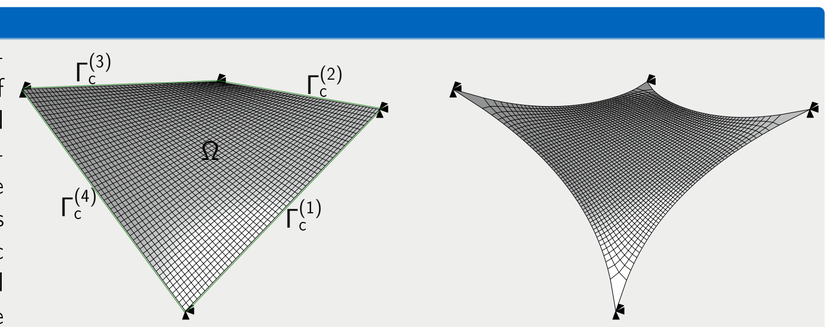

(a) Single patch design of a four point sail (b) Form-found shape of a single patch four point sail

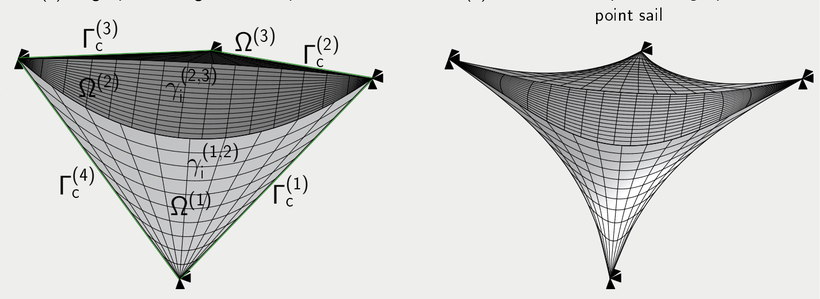

(c) 3-patch design of a four point sail (d) Form-found shape of a 3-patch patch four point sail using Nitsche

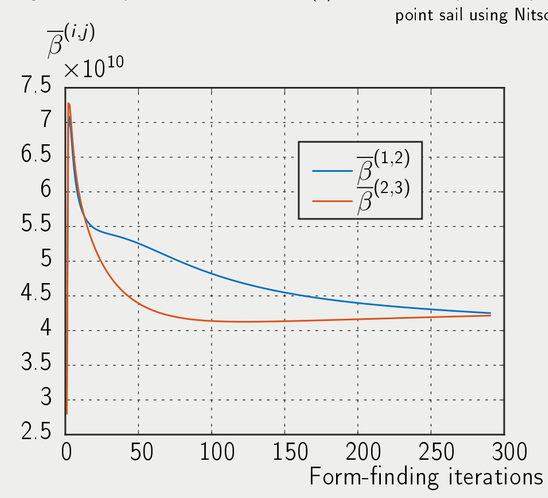

(e) Evolution of the stabilization parameters through the form-finding iterations

Figure 3: Form-finding analysis for both a single and a multipatch four point sail

Main sail of a sailing boat

A model of the main sail of a sailing boat is herein used as a second example. Subsequently, the geometry is divided into two patches as shown in Fig. 4(a). The Young's modulus, the poisson's ratio and the density of the sailcloth are chosen as $E = 1.8$ GPa, $\nu = 0.3$ and $\rho = 1150$ Kg/m, respectively. The thickness of the sail is $t = 1$ mm. Subsequently, the prestress is assumed isotropic of magnitude $n_0 = 10^2$Pa. Two cables are embedded on the sail's boundaries, with the same material properties as for the sailcloth but with ten times higher prestress. For patch 1 bi-cubic elements are employed whereas for patch 2 biquadratic. A modal analysis of the corresponding geometrically linear problem is performed and some of the resulting eigenmodes are shown in Fig. 4(c)-4(j) for both the single- and the multipatch settings. A transient analysis is subsequently performed using the Bossak time integration scheme between the time interval $[-6\,\text{s}, 18\,\text{s}]$ and the 2-norm of the displacement of the sailcloth's centroid through the time is shown in Fig. 4(b). For the coupling of the different patches along their common interfaces as well as the application of weak Dirichlet boundary conditions the Penalty, the Lagrange Multipliers and the Nitsche method are employed. For the given discretization all coupling methods yield identical results which demonstrate a phase shift when compared to the results from the single patch analysis which can be attributed to the spatial discretization. In what concerns the coupling properties, for the Penalty method the corresponding Penalty parameters are chosen as $\overline{\beta} = 7.905 \times 10^8$ and $\widetilde{\beta} = 4.722 \times 10^5$ by scaling the material matrix of the problem with the minimum element sizes. In what concerns the Lagrange Multipliers method, the number of elements concerning the Lagrange Multipliers discretization for the patch interface are chosen the same as for patch 1 along the interface and for the Dirichlet boundary the $\lceil 3/4 \rceil$ of the elements of each patch at the boundary. Contrary to the previously mentioned methods, no parameter has to be chosen for the Nitsche method.

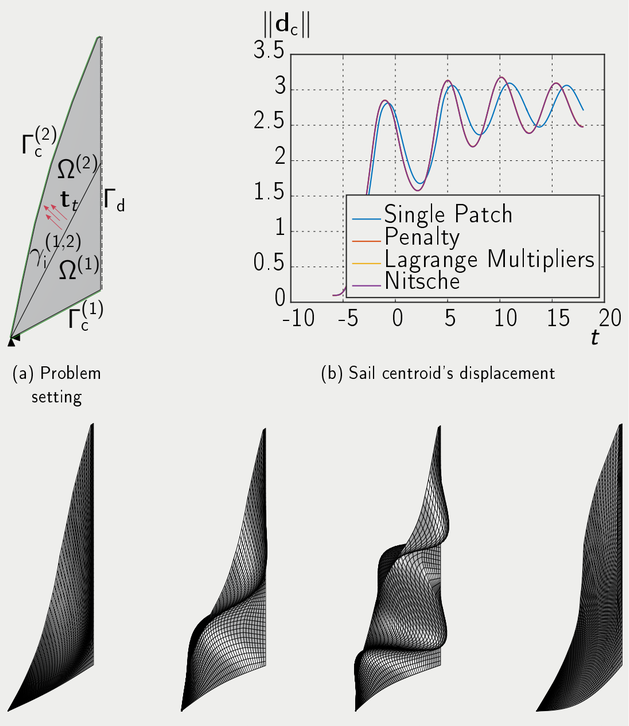

(a) Problem setting (b) Sail centroid's displacement

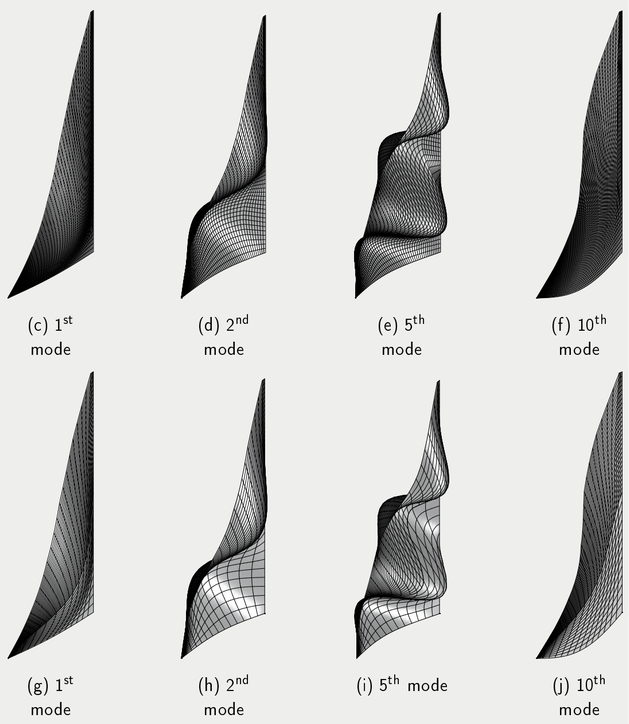

(c) 1st mode (d) 2nd mode (e) 5th mode (f) 10th mode

(g) 1st mode (h) 2nd mode (i) 5th mode (j) 10th mode

Figure 4: Modal and transient analysis for a sailcloth

References

- J.A. Cottrell, T.J.R. Hughes, and Y. Bazilevs. *Isogeometric Analysis: Toward Integration of CAD and FEA*. Wiley, 2009.
- Y. Basar and W. Krätzig. *Mechanik der Flächentragwerke*. Vieweg, Braunschweig, 1985.
- A. Apostolatos et al. "A Nitsche-type formulation and comparison of the most common domain decomposition methods in isogeometric analysis". In: *International Journal for Numerical Methods in Engineering* (2013).
- A. Apostolatos et al. "Isogeometric Analysis and Applications 2014". In: Springer International Publishing, 2015. Chap. Domain Decomposition Methods and Kirchhoff-Love Shell Multipatch Coupling in Isogeometric Analysis.
- K.-U. Bletzinger and E. Ramm. "Structural optimization and form finding of light weight structures". In: *Computers & Structures* 79 (2001), pp. 2053 –2062.

*E-mail: andreas.apostolatos@tum.de †http://empire.st.bv.tum.de, Lehrstuhl für Statik Prof. Dr.-Ing. K.-U. Bletzinger http://www.st.bgu.tum.de